International Journal of Electrical Engineering.
ISSN 0974-2158 Volume 4, Number 3 (2011), pp. 311-328

http://www.irphouse.com

An Enhanced Control Algorithm for Three Phase Shunt Triggering Compensator

[1]V.V. Karthikeyan and [2]B.R. Gupta

[1]A.P., Dept. of EEE, Kongu Engg. College, Perundurai, Tamilnadu-638052, India.
E-mail: karthi_maharaja@yahoo.com
[2]Senior Member, IEEE, India
E-mail: brgupta@ieee.org

Abstract

The reference signals estimation for shunt triggering compensator (STC), as thereby improving the power quality is the main objective of this paper and are derived by using time-scaling (wavelet transform) method is proposed in this paper. The traditional instantaneous reactive power theory (p-q theory) and linear convolution methods are adopted. The window selection is based on comparison of relative side-lope attenuation and leakage factor of various windows and the mother wavelet selection is based on comparison of retained energy level of input signal after compression by using various wavelets. A wavelet coefficient shrinkage (threshold) technique is also adopted in this paper. The proposed method has been verified and validated with MATLAB-SIMULINK model, signal processing and wavelet toolboxes.

Keywords: Shunt Triggering Compensator (STC), PQ Theory, Convolution, 1D-Wavelet Transform, Threshold, Decomposing.

Introduction

The power quality i.e., actually the voltage quality is being addressed in most cases [1]. Of course, in any practical power system there is a close relationship between voltage and current. In generating stations, all the generators should provide nearly perfect sinusoidal voltage, the current passing through system impedance causes variety of disturbances to the supplied voltage. For example, short circuit current cause the voltage to sag/dip, currents from lighting stroke passing through the system impedance cause high-impulse voltage that leads to short circuit, harmonic currents (distorted currents) produced by commercial loads (such as single phase SMPS, high-efficiency fluorescent lightning with electronic ballast, air-conditioning, etc.,) and

industrial loads (such as three phase converter based ac and dc drives, arc furnaces, etc.,) can distort the supply voltage. The economic impact on industrial customers is directly related to power quality variations. Modern days many industries are semi/fully automated and equipped with sensitive electronic control devices. These devices are much more sensitive to the supply voltage variations. Hence, to reduce the harmonic currents (due to non-linear loads), thereby improving the power quality, a three phase STC is presented in this paper. The STC can effectively compensate (i.e., injecting equal energy in-phase opposition to that of harmonic content) the high frequency harmonic currents. Many methods have been used to generate the compensating currents for STC, which are proposed in literature. For example, frequency domain [2][3], time domain [4][5], time-frequency domain [6] and time-scaling [7]. In frequency domain, the time information is lost and in time domain, the frequency information is lost. In order to get the time and frequency information of any signal (such as harmonics, flicker, sag, swell, noise, notching, etc.,) the methods [6][7] have been used.

We approached time-scaling method to extract the reference current signals for STC. The sampled input signal is convolved with a pre-defined window function and the resulting signal is decomposed (i.e., 1D-wavelet transform) by a selected wavelet function to get the reference current signals. Finally the results of balanced and unbalanced source voltages conditions are compared. The time domain (p-q theory) approach [5], which is given in the next section.

P-q Theory

The instantaneous real and reactive powers are proposed in literature [8]-[20] and are derived from Clarke transformation. The compensating powers and corresponding compensating currents are calculated based on p-q theory and are given in (1)-(10) & (11)-(12):

$$\begin{pmatrix} V_0 \\ V_\alpha \\ V_\beta \end{pmatrix} = (\sqrt{2/3}) \begin{pmatrix} 1/\sqrt{2} & 1/\sqrt{2} & 1/\sqrt{2} \\ 1 & -1/2 & -1/2 \\ 0 & \sqrt{3}/2 & -\sqrt{3}/2 \end{pmatrix} \begin{pmatrix} V_a \\ V_b \\ V_c \end{pmatrix} \quad (1)$$

$$\begin{pmatrix} V_a \\ V_b \\ V_c \end{pmatrix} = (\sqrt{2/3}) \begin{pmatrix} 1/\sqrt{2} & 1 & 0 \\ 1/\sqrt{2} & -1/2 & \sqrt{3}/2 \\ 1/\sqrt{2} & -1/2 & -\sqrt{3}/2 \end{pmatrix} \begin{pmatrix} V_0 \\ V_\alpha \\ V_\beta \end{pmatrix} \quad (2)$$

$$V_{a(t)} = \sqrt{2}V\cos(\omega t) \;\; ; \;\; V_{b(t)} = \sqrt{2}V\cos(\omega t - 2\pi/3)$$
$$V_{c(t)} = \sqrt{2}V\cos(\omega t + 2\pi/3) \quad (3)$$

$$i_{a(t)} = \sqrt{2}I\cos(\omega t + \phi) \;\; ; \;\; i_{b(t)} = \sqrt{2}I\cos(\omega t + \phi - 2\pi/3)$$
$$i_{c(t)} = \sqrt{2}I\cos(\omega t + \phi + 2\pi/3) \quad (4)$$

$$V_\alpha = \sqrt{3}V\cos(\omega t) \qquad i_\alpha = \sqrt{3}I\cos(\omega t + \phi)$$
$$V_\beta = \sqrt{3}V\sin(\omega t) \qquad i_\beta = \sqrt{3}I\sin(\omega t + \phi) \quad (5)$$

$$V_\alpha = \sqrt{3}V\cos(\omega t) \qquad i_\alpha = \sqrt{3}I\cos(\omega t + \phi)$$
$$V_\beta = \sqrt{3}V\sin(\omega t) \qquad i_\beta = \sqrt{3}I\sin(\omega t + \phi) \qquad (5)$$

$$\begin{pmatrix} P_0 \\ P \\ q \end{pmatrix} = \begin{pmatrix} V_0 & 0 & 0 \\ 0 & V_\alpha & V_\beta \\ 0 & V_\beta & -V_\alpha \end{pmatrix} \begin{pmatrix} i_0 \\ i_\alpha \\ i_\beta \end{pmatrix} \qquad (6)$$

$$P_{3\phi}(t) = v_a i_a + v_b i_b + v_c i_c = v_\alpha i_\alpha + v_\beta i_\beta + v_0 i_0 \qquad (7)$$

$$q = V_\alpha J i_\beta + V_\beta J i_\alpha \qquad (8)$$

Convolution

The response of the filter can be identified by using convolution theorem. According to this theorem, if two signals are multiplied in time domain, the resulting product frequency response is equal to the convolution of individual frequency responses. Thus, multiplication of signals in one domain is equal to convolution in other domain. While designing a low-pass filter, the window method is opted instead of Fourier series method.

Because in the latter method to obtain the impulse response, abrupt truncation of desired impulse response has to be done, which leads to more oscillations in pass-band and stop-band in the frequency spectrum of ideal low-pass filter. The window selection is based on some desirable characteristics [21], such as the width of main-lope should be small and it should contain as much of total energy as possible. In our case, some additional characteristics of windows, such as their relative side-lope attenuation and leakage factor are also taken into consideration. Table.1 consists of various windows and its desirable characteristics for the input sample, which has the length of 1024 and is calculated by using MATLAB- window design & analysis tool. From the above Table.1, we found two windows, such as; chebyshev and flat-top are inverse proportionality in their relative side-lope attenuation and leakage factor. We analyzed both the cases.

Table 1: Window Types and its desirable characteristics.

Window Type	No. Of samples	Main Lope width in db	Relative side lope attenuation in db	Leakage factor in %
Bartlett	1024	-3	-26.5	0.28
Bartlett-Hanning	1024	-3	-35.9	0.03
Blackman	1024	-3	-58.1	0.00
Blackman-Harris	1024	-3	-92.1	0.00
Bohman	1024	-3	-46.0	0.00
Chebyshev	1024	-3	-100	0.00
Flat-Top	1024	-3	0.0	97.47
Gaussian	1024	-3	-43.8	0.01
Hamming	1024	-3	-42.6	0.03
Hanning	1024	-3	-31.5	0.05

Kaiser	1024	-3	-13.6	8.48
Nuttall	1024	-3	-95.7	0.00
Parzen	1024	-3	-53.0	0.00
Rectangular	1024	-3	-13.3	9.26
Taylor	1024	-3	-30.3	0.44
Triangular	1024	-3	-26.5	0.28
Tukey	1024	-3	-31.5	0.05

1-D Wavelet Transform

1-D Wavelet transform is a good choice for analyzing the power signals. Some papers in literature [22] [23] [24] [25] are proposed WT to analyze harmonics on the power system. Firouzah [7] proposed WT based controller for shunt active power filter using synchronous fundamental dq-frame, orthogonal wavelet and hamming window. We proposed 1-D WT based controller for three phase shunt active power filter using instantaneous pq-theory. The mother wavelet selection is based on the retained energy level of the input signal after compression and is calculated from MATLAB-wavelet toolbox. Table.2 clearly indicates that, the bi-orthogonal6.8 wavelet has retained the energy of input signal more compared to Daubechies and D-Meyer wavelets. Hence, we chose bi-orthogonal6.8 is our mother wavelet to decompose the input signal (load current). To identify the fundamental component from the load current is based on the transformation of time-varying signal or distorted signal into time-scale signal using a mother wavelet function Ψ(t) and is given in (13):

Table 2: Retained Energy level of Input signal.

Wavelet Level	Threshold (T)	Retained Energy after compression in %			
		db8	db20	Dmey	bior6.8
1(cD10)	1.73	99.87	99.82	99.87	99.92
2(cD9)	2.08	99.84	99.75	99.83	99.88
3(cD8)	2.63	99.75	99.63	99.75	99.83
4(cD7)	3.12	99.67	99.50	99.69	99.76
5(cD6)	4.02	99.48	99.23	99.50	99.60
6(cD5)	4.99	99.23	98.95	99.23	99.46
7(cD4)	6.03	99.00	98.70	99.06	99.25
8(cD3)	6.86	98.79	98.44	98.93	99.13
9(cD2)	8.04	98.52	98.17	98.61	98.89
10(cD1)	9.01	98.26	97.96	98.37	98.69

$$\Psi(t) = \sqrt{2}\ \sum_s h(s)\phi(2t - s) \tag{13}$$

Where $\phi(t)$ is called scaling function and is given in (14):

$$\phi(t) = \sqrt{2}\ \sum_s l(s)\phi(2t - s) \tag{14}$$

In (13) and (14), h(s) and l(s) are coefficients of high-pass filter and low-pass filter respectively. The two phase system load currents $i_\alpha(t)$ and $i_\beta(t)$ with the sample length of 1024 are decomposed at various scales of resolutions by using a mother wavelet function as given in (13). At scale1, the sampled signal $i_\alpha(s)$, is decomposed into the signals *cA1(s)* and *cD1(s)* that are the approximation and detail of the signal respectively and defined in (15) and (16):

$$cA1(s) = \sum_k l(k-2s) i_\alpha(k) \quad (15)$$

$$cD1(s) = \sum_k h(k-2s) i_\alpha(k) \quad (16)$$

Where k is the steady state sample. Due to the strength reduction process, if the signal $i_\alpha(t)$ has N samples, then the level1 approximation (*cA1)* and detailed (*cD1*) coefficients will have only N/2 samples. The same process is repeated up to the number of levels is chosen (for our case, we chose number of levels of decomposition is 10). By filtering technique, the resolution is changed and also the scale is altered by either *up-sampling* or *down-sampling* by 2. This concept is shown in Fig.1 and it is called sub-band coding.

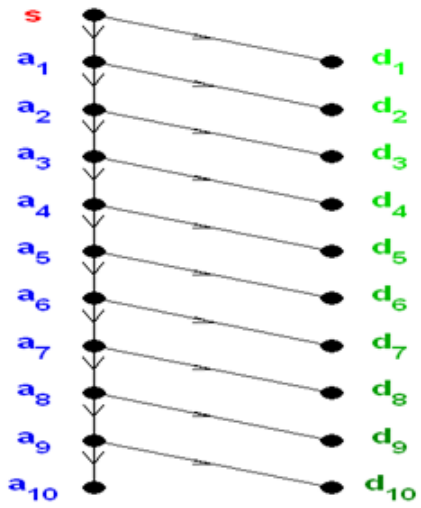

Figure 1: Ten level wavelet decomposition Tree.

The frequency bands corresponding to each level [25] is determined as in (17):

$$Fj = (f_s/2^{j+1}),\ j=1,2,\ldots M \quad (17)$$

Where Fj is the higher limit of the frequency band represented by the level j, M is the number of scales and F_M is the bandwidth of the filter that calculates the approximated co-efficient (cA1 to cA10) and detailed co-efficient (cD1 to cD10), which are given in Table.3 and f_s is the sampling frequency (we chose f_s = 10.24KHz).

Table 3: Frequency Band and Harmonic Order for Each Scale or Level.

Sl.no	Wavelet level (co-efficient)	Frequency band (Hz)	Middle frequency (Hz)	Harmonic order
1	10(cA10)	DC – 5	3.75	Less than Fundamental (Inter-harmonics)
2	10(cD10)	5 – 10	7.5	
3	9(cD9)	10 – 20	15	
4	8(cD8)	20 – 40	30	
5	7(cD7)	40 – 80	60	Fundamental & 1.5 (Inter-harmonics)
6	6(cD6)	80 – 160	120	Fundamental & 1.5, 3
7	5(cD5)	160 – 320	240	3- 7
8	4(cD4)	320 – 640	480	7 – 13
9	3(cD3)	640 – 1280	960	13 – 25
10	2(cD2)	1280 – 2560	1920	25 – 51
11	1(cD1)	2560 – 5120	3840	51 – 103

The middle or centre frequency M_j of the filter at scale j as given in (18):

$$M_j = 3f_s/2^{j+2} \text{ j=1,2……M} \quad (18)$$

Wavelet coefficient shrinkage (threshold) technique

The proposed method is based on decomposing the load current signals ($i_\alpha(t)$ and $i_\beta(t)$) into ten levels of 1D-Wavelet Transform. Initially, the load currents are synthesized (de-noised by shrinkage) through a threshold value T can be determined using the universal thresholding which was proposed by Johnstone Donoho [23], which removes the coefficients below a threshold value, then taking the Inverse DWT (IDWT) as given in (19):

$$T = \sigma\sqrt{2(\log(N)} \quad (19)$$

Where T is threshold, N is the half of sample data length and σ is the noise standard deviation as given in (20):

$$\sigma = \text{Median}(|cD|) / 0.6745 \quad (20)$$

Where cD is the detailed coefficient for each level.
If the scale is large [24], then the threshold equals as in (21):

$$T_m = C_m \ln(L) \quad (21)$$

Where the constants C_m as given in Table.4 and L is the length of data. If the scale is small, m<<P-1 (where P=L/K; L - Total data length and K- selectable data length), then the threshold as given in (22):

$$T_m = \frac{\pi}{\sqrt{3}}\sqrt{\ln(N)} \quad (22)$$

For each level from 1 to j, a threshold value is selected through a loop and it is applied for the detailed coefficients of the signal as obtained in each level of decomposition.

Table 4: Various values of C_m for determining the Threshold.

Scale m	C_m	Scale m	C_m
P-1	1.30	P-6	0.58
P-2	1.16	P-7	0.45
P-3	0.99	P-8	0.38
P-4	0.87	P-9	0.30
P-5	0.72	P-10	0.25

This is able to remove the noise and achieve high compression ratio because of the concentrating ability of the wavelet transform. The chosen threshold value for each level gives the minimum error between the detailed coefficients (of harmonics) and those of original signal. We use higher wavelet scales, hence the threshold value for each level is calculated from (21) and which are given in Table.5.

Table 5: Threshold values for each level.

Wavelet level	Threshold (T)	Wavelet level	Threshold (T)
1(cD10)	1.73	6(cD5)	4.99
2(cD9)	2.08	7(cD4)	6.03
3(cD8)	2.63	8(cD3)	6.86
4(cD7)	3.12	9(cD2)	8.04
5(cD6)	4.02	10(cD1)	9.01

Proposed Controller

The proposed method of WT based controller for STC is shown in Fig.3. The reference currents are obtained from wavelet transform method is injected in opposition to that of harmonic current present in the source current by STC using predictive current control method (i.e., hysteresis current control). To verify the proposed method, MATLAB-SIMULINK has been used and tested with a rectifier load and various supply voltages conditions. Fig.4 shows the general scheme of compensated system using wavelet transform. The method of generating the reference currents for STC is explained in the following steps:

1. **Signal Extraction:** The three phase load currents I_{la}, I_{lb}, I_{lc} are first transformed from three phase system into two phase system currents $i_{\alpha}(t)$, $i_{\beta}(t)$

and i_0 using proposed pq model. The alpha and beta axis currents do not contain zero sequence current. Hence, the fundamental components of i_α and i_β are extracted by the proposed technique.

2. **Sampling:** The $i_\alpha(t)$ and $i_\beta(t)$ currents are sampled and collected as a signals $i_\alpha(s)$, $i_\beta(s)$ with a length of 2^n (n – no. of samples). Here, we assume n=10, hence the number of collected samples are 1024 during the observation period of 100ms is shown in Fig.2.

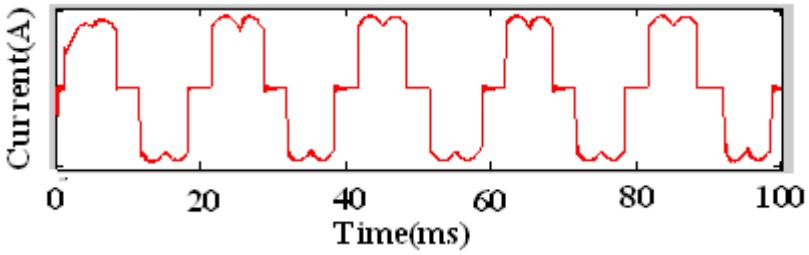

Figure 2: Load Current I_{la}.

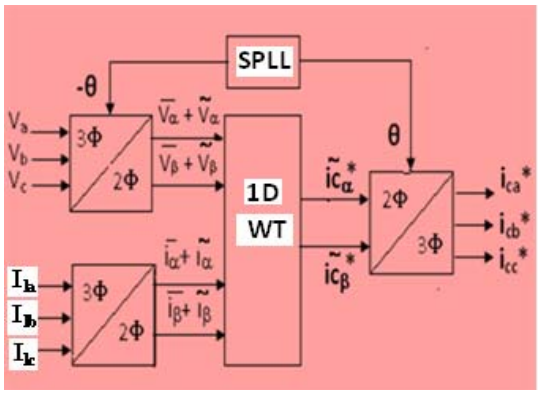

Figure 3: Proposed Method.

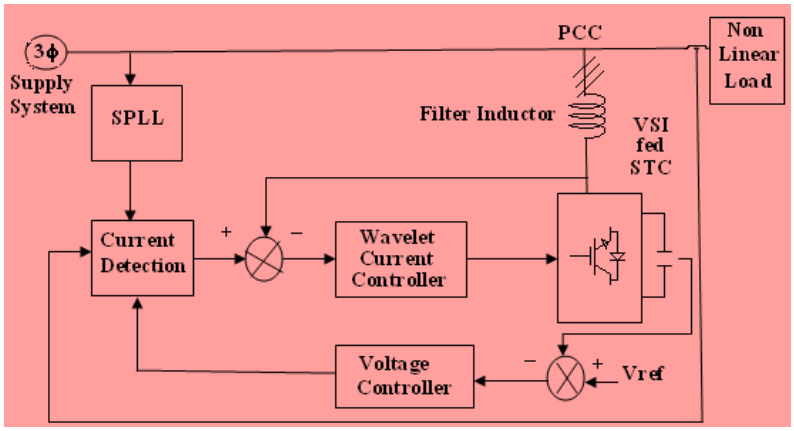

Figure 4: Schematic diagram of STC.

Thus the sampling frequency is 10240Hz. The maximum frequency (F_{max}) that can be measured is given by the Nyquist theory as in (23):

$$F_{max} = f_s/2 \tag{23}$$

Where f_s is sampling frequency.

3. **Convolution:** A 1024 samples of the proposed chebyshev and flat-top windows are convolved with the sampled load currents separately.
4. **Decompose:** A ten level WT ($K=2^j$, where K is the total number of data points and j is the number of levels) is used to decompose the resulting convolution signal, which consists of 4h±1 and 6h±1 order harmonics, where h is positive integer.
5. **Reconstruction:** The original signal is reconstructed by IDWT i.e., reconstruction is done by using the original approximation coefficient of level 10 (cA10) (i.e., extracted fundamental current) and the modified detail coefficients of levels from 1 to *10 (cD1 to cD10).*
6. **Reference signals:** The two phase harmonic currents $\widetilde{i_{c\alpha}^*}$ and $\widetilde{i_{c\beta}^*}$ are then obtained by subtracting the extracted fundamental currents $i_{\alpha f}$ and $i_{\beta f}$ from the two phase load currents $i_\alpha(s)$ and $i_\beta(s)$ respectively and are given in (24):

$$\widetilde{i_{c\alpha}^*} = i_{\alpha f} - i_\alpha(s)\ ;\ \widetilde{i_{c\beta}^*} = i_{\beta f} - i_\beta(s) \tag{24}$$

Finally, these two-phase harmonic components are transformed into three phase system using pq model as given in (12). The three phase currents i_{ca}*, i_{cb}*, i_{cc}* obtained after inverse Clarke transformation are then used as a reference signals for hysteresis current controller, to generate gating signals for STC.

7. Synchronization: The synchronization between the injected signal and the actual source signal can be done by soft phase loop lock (SPLL) [26]. When $\widetilde{i_{c\alpha}^*}$ is set to zero, then the calculated θ is synchronous with the fundamental voltage positive-sequence component. When $\widetilde{i_{c\alpha}^*}$ is not set to zero, an adequate phase difference (which is not affecting the selected harmonic detection and elimination) is between θ and the positive-sequence component of fundamental voltage, which make the control of the displacement factor easy.

Simulation Conditions and Results

Case 1: Supply Voltages Condition – Balanced; Window type – Chebyshev; Wavelet –biorthogonal6.8

Fig.5 shows the proposed WT method and reconstruction process to extract phase-a fundamental component (50Hz). Fig.6 shows the FFT analysis of I_{la} (before compensation) mainly contains 6h±1 order harmonics, where h is positive integral. From the FFT analysis, we conclude that most dominating harmonics for our case are 5^{th}, 7^{th}, 11^{th} and 13^{th} order, while 3^{rd} and 9^{th} order harmonics are least dominating

because of its angle of rotation from the fundamental is 39.5° and 182.3° respectively. Fig.7 shows the FFT analysis of I_a (after compensation) clearly indicates that the proposed algorithm is versatile for detecting and eliminating the lower-order harmonic well. The approximate component cA10 will remove harmonics and only contain fundamental and cD1– cD6 contains high-frequency harmonics, whereas cD7-cD10 contains fundamental and inter-harmonics. Due to the presence of 5^{th} order harmonics (THD level of 22.47%) signal present in cD10 contrasting with one cycle (20ms) in cA10. Fig.8 shows phase-a harmonics current (non-sinusoidal current or reference current i_{ca}*) is obtained by WT, which is generated by subtracting extracted fundamental components current i_{af} from practical load current $I_{la.}$

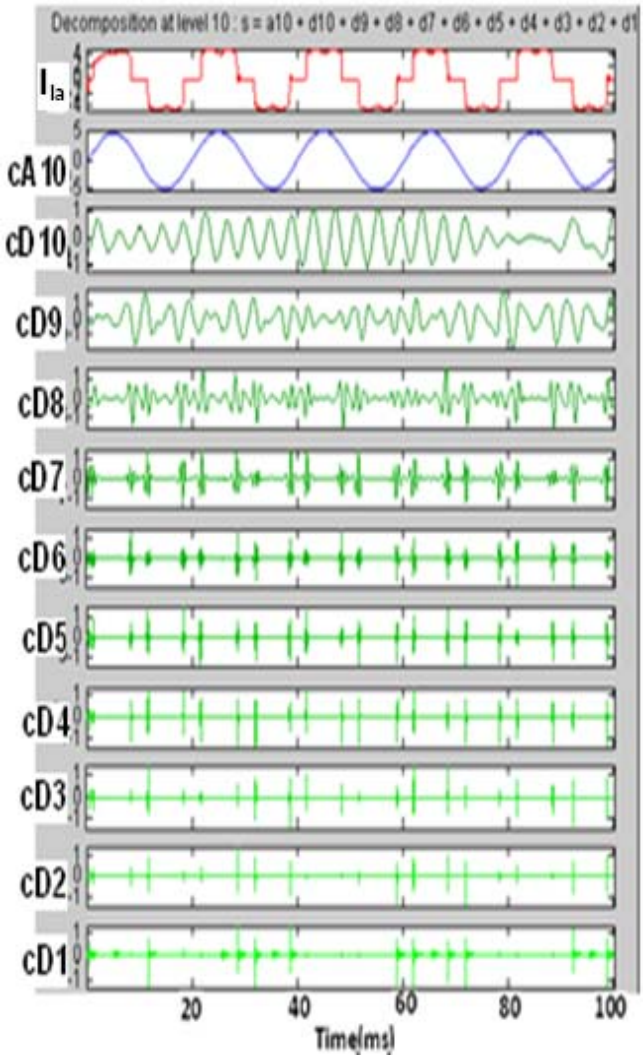

Figure 5: Ten- level Bi-orthogonal WT to load current $Il_{a.}$

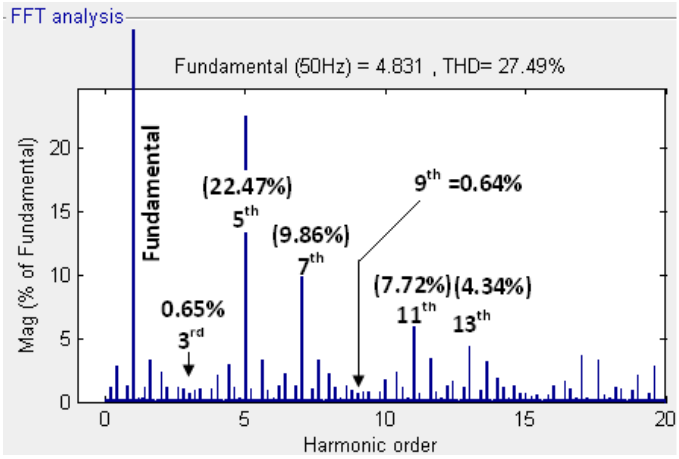

Figure 6: FFT spectrum analysis load current I_{la} (Before compensation).

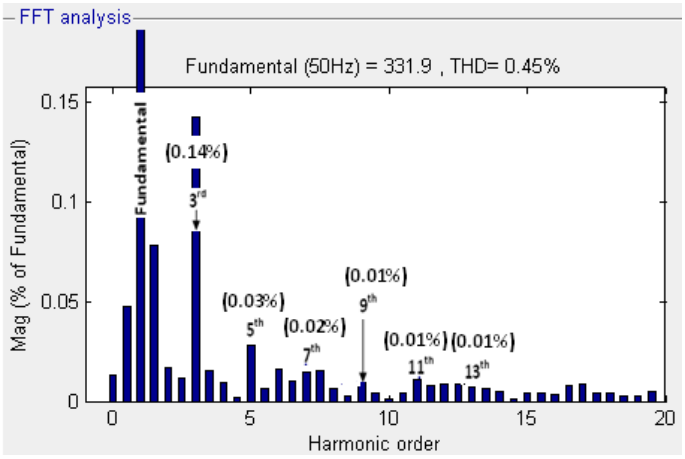

Figure 7: FFT spectrum analysis for source current I_a (After compensation).

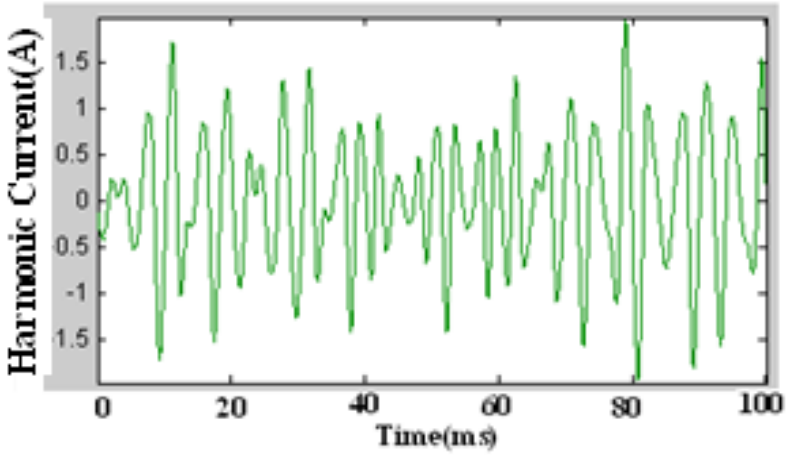

Figure 8: Phase-a Harmonic current using WT method.

Fig.9 shows calculated phase-a fundamental current i_{af} using bi-orthogonal6.8 wavelet with balanced mains voltage conditions. Fig.10 shows the simulation results of the proposed controller under the mains voltages are balanced condition.

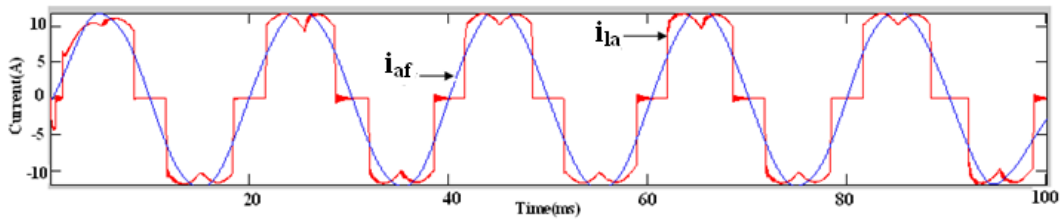

Figure 9: Calculated Phase-a fundamental current i_{af} using bi-orthogonal6.8 wavelet.

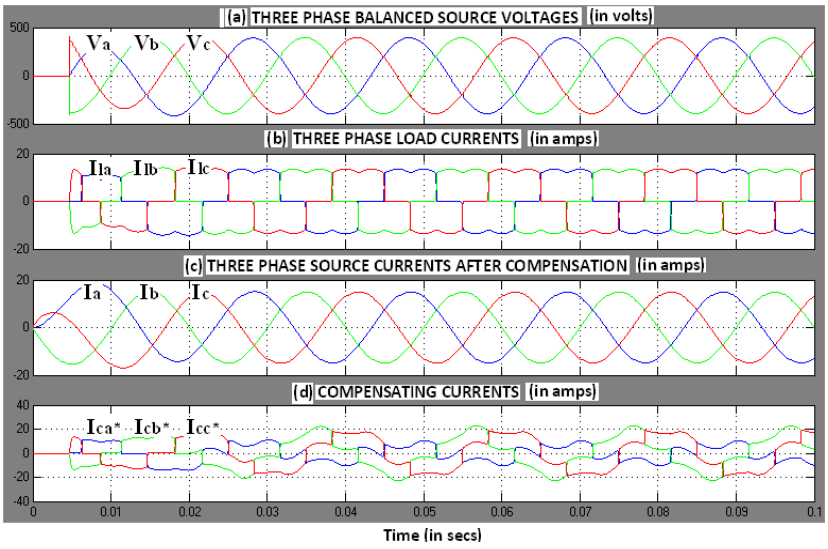

Figure 10: Simulation Results of (a) Three phase balanced source voltages (b) Three phase load currents (i.e., Source currents before compensation) (c) Three phase source currents after compensation (d) Compensating currents before compensation.

Case 2: Supply Voltages Condition – Unbalanced; Window type – Chebyshev; Wavelet – biorthogonal6.8

Fig.11 shows the FFT analysis of I_{la} (before compensation) mainly contains 4h±1 order harmonics, where h is positive integral. From the FFT analysis, we conclude that most dominating harmonics for our case are 3rd to 25th order, while 11th order harmonic is the least dominating because of its angle of rotation from the fundamental is 181.2°. Fig.12 shows the FFT analysis of I_a (after compensation) clearly indicates that the proposed algorithm is versatile for detecting and eliminating the lower-order harmonics, especially 3rd, 5th, 7th and 9th and also for higher order harmonics. Fig.13 shows the simulation results of the proposed controller under the mains voltages are unbalanced condition.

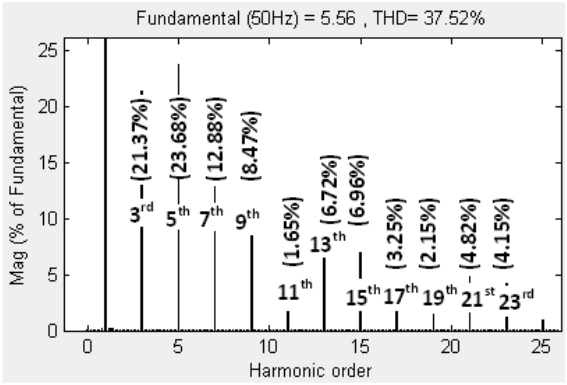

Figure 11: FFT spectrum analysis load current I_{la} (Before compensation).

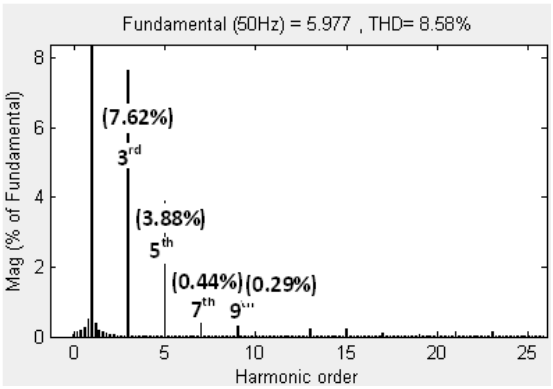

Figure 12: FFT spectrum analysis for source current I_a (After compensation).

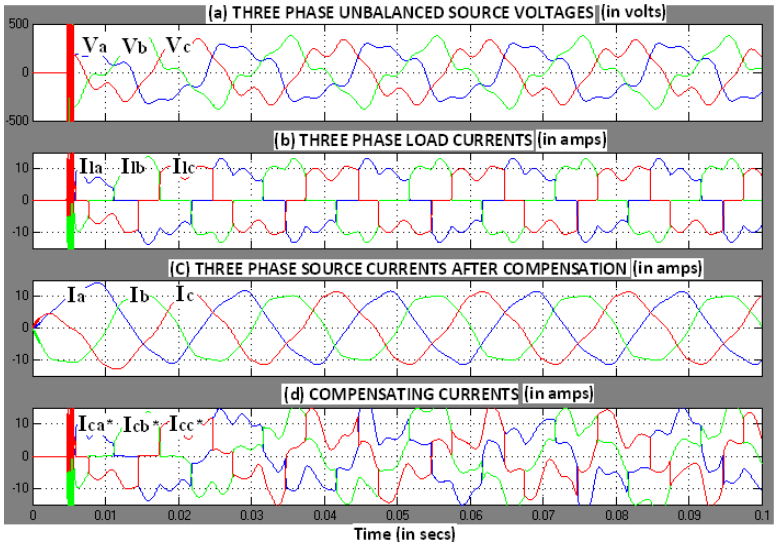

Figure 13: Simulation Results of (a) Three phase unbalanced source voltages (b) Three phase load currents (i.e., Source currents before compensation) (c) Three phase source currents after compensation (d) Compensating currents before compensation.

Case 3: Supply Voltages Condition – Balanced; Window type – Flat-Top; Wavelet – biorthogonal6.8

Fig.14 shows the FFT analysis of I_{la} (before compensation) mainly contains 6h±1 order harmonics, where h is positive integral. From the FFT analysis, we conclude that most dominating harmonics for our case are 5^{th}, 7^{th} and 11^{th}, while 9^{th} order harmonic is the least dominating because of its angle of rotation from the fundamental is 165.3°. Fig.15 shows the FFT analysis of I_a (after compensation) clearly indicates that the proposed algorithm is versatile for detecting and eliminating the lower-order harmonics.

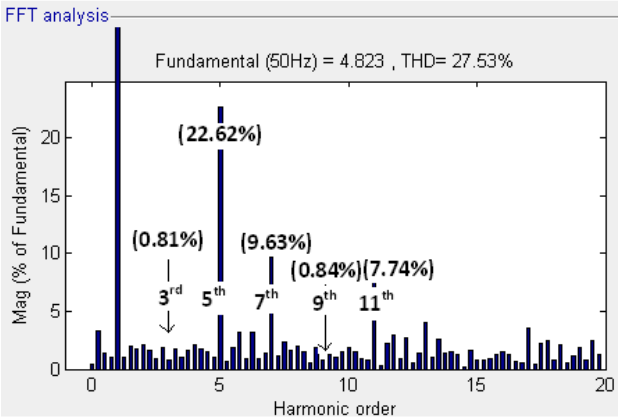

Figure 14: FFT spectrum analysis load current I_{la} (Before compensation).

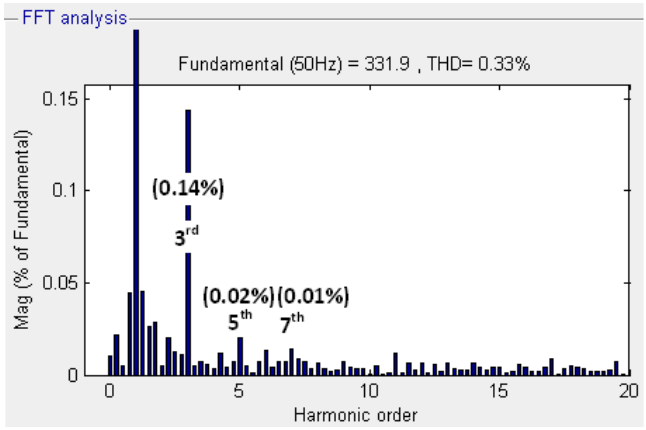

Figure 15: FFT spectrum analysis for source current I_a (After compensation).

Case 4: Supply Voltages Condition – Unbalanced; Window type – Flat-Top; Wavelet – biorthogonal6.8

Fig.16 shows the FFT analysis of I_{la} (before compensation) mainly contains 4h±1 order harmonics, where h is positive integral. From the FFT analysis, we conclude that most dominating harmonics for our case are 3^{rd} to 15^{th}. Fig.17 shows the FFT

analysis of I_a (after compensation) clearly indicates that the proposed algorithm using flat-top window under unbalanced voltages condition is lesser response comparing the chebyshev window method and also the THD of source current I_a is 25.87% after compensation.

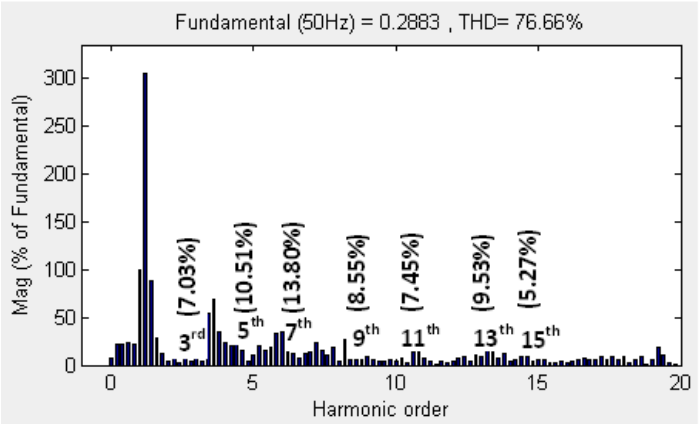

Figure 16: FFT spectrum analysis load current I_{la} (Before compensation).

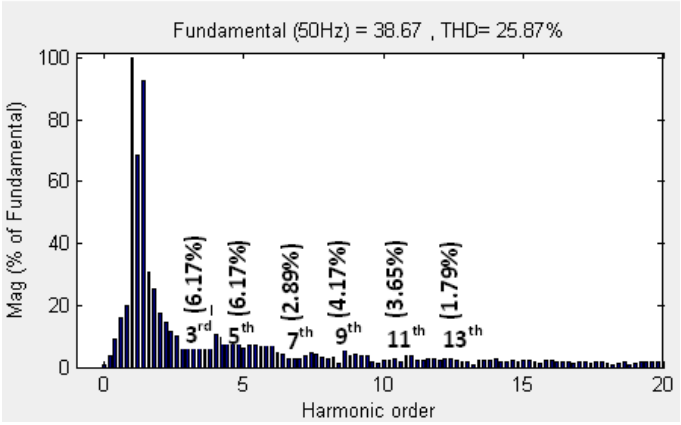

Figure 17: FFT spectrumanalysis for source current I_a (After compensation).

Conclusion

Most of the power conditioning units uses power electronic components, results in distorted voltages at point of common coupling. Also un-even distribution of load leads to current un-balance in three phase, four wire system. This paper gives a complete account of the application of the 1D-wavelet transform for draw-out of fundamental component from the load current in-order to generate the reference currents for shunt triggering compensator. The proposed controller was designed and tested by using MATLAB software based on inverse proportionality characteristics of windows. The entire model in αβ-coordinates is presented. Finally, simulation results for balanced and unbalanced source voltage conditions were obtained to show the

effectiveness of the proposed control method. The proposed method can be used for real-time monitoring and compensation of power quality problems, such as harmonics, noises, inter-harmonics, sag, swell etc.,.

References

[1] Roger C.Dugan., 2008, Electrical power systems quality, Edition: 2 (McGraw-Hill).

[2] Budeanu, C.I., 1927, "The different options and conceptions regarding Active power in Non-sinusoidal systems," Instytut Romain de I'Energie, Bucharest, pub.no.4.

[3] Jose Maria Ortega., 2005, "Reference current computation methods for active power filters: Accuracy assessment in the frequency domain," IEEE Trans.on.power.Del.,Vol.20, no.2, pp.446-456.

[4] Fryze, S., 1931, "Active, reactive and apparent powers in systems with distorted waveform," Prz.Elektrotech., Z.7, pp.193-203, Z.8, pp.225-234.

[5] Watanabe, E.H., Akagi, H., and Aredes, M., 2008, "Instantaneous p-q power theory for compensating non-sinusoidal systems," IEEE Transactions., pp.195-201.

[6] Walid.G.Morsi., and El-Hawary, M.E., 2007, "Time-Frequency non-sinusoidal current decomposition based on the wavelet packet transform," IEEE ., ISBN: 1-4244-1298-6.

[7] Firouzjah, K.G.,and Sheikholeslami, A., 2008, "A New harmonic detection method for shunt active filter based on wavelet transform," Journal of applied sciences research, 4(11), pp.1561-1568.

[8] Mishra, M.K., Joshi, A., and Ghosh, A., 2001, "Unified shunt compensator algorithm based on generalized instantaneous reactive power theory," IEEE Trans. Gen., Distrib., Vol.148, no.6, pp.583-589.

[9] Watanabe, E., and Aredes, M., 2000, "Compensation of non-periodic currents using the instantaneous reactive power theory," Proc. Power Eng. Soc. Summer Meeting, Vol.2, pp.994-999.

[10] Arrillaga, J., and Watson, N.R., 2001, Power system quality assessment, (New York: John Wiley & Sons).

[11] Clarke, E., 1943, Circuit Analysis of AC Power Systems – Symmetrical and Related Components, Vol.1, (New York: John Wiley & Sons).

[12] Watanabe, E.H., Arades, M, and Akagi, H., 2002, "The p-q Thoery for Active Filter Control: Some Problems and Solutions," In: 14th Conferences of Automatic, Natal – RN, Brazil, pp.1078-1083.

[13] Salmeron, P., and Montano, J.C., 1996, "Instantaneous power components in poly phase systems under non-sinusoidal conditions," Proc. Inst. Elect. Eng. Sci., Meas., Technol., Vol.143, no.2, pp.239-297.

[14] Morendaz-Eguilaz, J.M., and Peracaula, J., 1999, "Understanding AC power using the generalized instantaneous reactive power theory: Considerations for

instrumentation of three-phase electronic converters," in Proc. IEEE Int. Symp .Ind. Elect., Vol.3, pp.1273-1277.

[15] Aller, J.M., 2000, "Space vector application in power systems," in proc.3rd IEEE Int. Conf. Devices, Circuits, Systems, pp.P78/1-P78/6.

[16] Aller, J.M., Bueno, A., and Restrepo, J.A., 1999, "Advantages of the instantaneous reactive power definition in three-phase system measurement," IEEE Power Eng. Rev., Vol.19, no.6, pp.54-56.

[17] Peng, F.Z., and Lai, J.S., 1996, "Generalized instantaneous reactive power theory for three-phase power system," IEEE Trans. Instru. Measurement, Vol.45, no.1, pp.293-297.

[18] Kim, K., Blaabjerg, F., and Jensen, B.B., 2002, "Spectral analysis of instantaneous power in single-phase and three-phase systems with use of p-q-r theory," IEEE Trans .Power Electron, Vol.17, no.5, pp.711-720.

[19] Czarnecki, L.S., 1998, "Orthogonal decomposition of the current in a three-phase nonlinear asymmetrical circuit with non-sinusoidal voltage," IEEE Trans. Instrumentation. Meas., Vol.IM-37, no.1, pp.30-34.

[20] Czarnecki, L.S., 1995, "Power related phenomena in three-phase unbalanced systems," IEEE Trans. Power. Del., Vol.10, no.3, pp.1168-1176.

[21] Ambardar, A., Digital Signal Processing: A Modern Introduction, THOMSON, pp: 380-381.

[22] Ghanbari, Y., and Karami-Mollaei, M.R., 2006, "A new approach for speech enhancement based on the adaptive thresholding of the wavelet packets". Speech Communication, 48: 927-940.

[23] Donoho, D.L., and Johnstone, M., "Ideal spatial adaption by wavelet shrinkage," in Biometrika, Vol.3, no.81, pp.425-455.

[24] Vidakovic, B., 1999, Statistical Modeling by Wavelets, First edition New Jersey: Wiley, pp.408 Probability and Statistics. ISBN 0-471-29365-2.

[25] YuHua Gu, and Bollen, M.H.J., 2000, "Time-Frequency and Time-scale Domain Analysis of Voltage Disturbances," IEEE Trans. On Power Delivery, Vol.15, no.4, pp.1279-1283.

[26] Kaura, V., and Blasko, V., 1997, "Operation of a phase locked loop system under distorted utility conditions," IEEE Trans. Ind. Appl., Vol. 33, no. 3, pp.58–63.

Authors Biography

Karthikeyan V.V. received his B.E degree in Electrical and Electronics Engineering from Maharaja Engineering College, Tamilnadu, India, in 2000 and received his M.E degree in Power Electronics from K.S.Rangasamy College of Tech, Tamilnadu, India, in 2007. In between he was a Lecturer at Sasurie College of Engineering. He is presently pursuing his Ph.D. under Anna University of Technolgy, Coimbatore, Tamilnadu. He is currently a Assistant Professor in Electrical Department, Kongu Engineering College, Erode, India. His research interests include power quality, power electronics and signal processing. He is a member in ISTE. Also he has published 10 papers in national and international conferences.

Gupta B.R. received his B.Sc (Engg) (Hons)., M.Sc(Egg) (Disn)., and Ph.D. degrees in Electrical Engineering from Punjab University, India, in 1961, 1967, and 1979 respectively. He was in PEC University of Technology, Chandigarh from 1961 to 1997. He is currently a visiting professor and consulting Engineer. He is a senior member IEEE and member IE (India). His research interests include power system, power quality and power electronics. He has published more than 100 transactions and conference papers. Also he has published many books which were recommended as a text book in various colleges and universities. He has received many awards for his research work.